

# Tensile and compressive deformation of polypyridobisimidazole (PIPD)-based ‘M5’ rigid-rod polymer fibres

J. Sirichaisit, R.J. Young\*

Manchester Materials Science Centre, UMIST/University of Manchester, Grosvenor Street, Manchester M1 7HS, UK

Received 19 February 1998; accepted 14 July 1998

## Abstract

The tensile and compressive deformation behaviour of a new type of heterocyclic rigid-rod polymer fibre, polypyridobisimidazole ‘PIPD’ or ‘M5’, produced by the spinning of liquid-crystalline solutions, have been studied. The Young’s moduli and tensile strengths for the two different PIPD or M5 fibres have been determined to be greater than 300 GPa and 4 GPa, respectively. Molecular deformation in the fibres has been monitored using Raman spectroscopy and it has been shown that the peak positions of the Raman bands in the fibres are sensitive to the application of mechanical stress and strain. This has enabled a detailed study of molecular deformation to be undertaken for both tensile and compressive deformation. Full tensile-compression stress–strain curves have been derived and the compressive modulus and compressive strength of the PIPD fibres have been determined to be greater than 300 GPa and up to 1 GPa, respectively, which are both considerably higher than values for other high-performance polymer fibres. The potential use of PIPD fibres as reinforcing fibres in high-performance composites is discussed. © 1999 Elsevier Science Ltd. All rights reserved.

**Keywords:** Raman spectroscopy; Poly(pyridobisimidazole) fibres; Molecular deformation

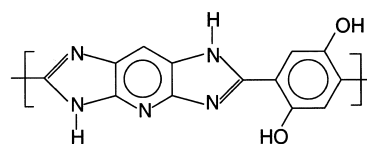
## 1. Introduction

High-performance polymeric fibres with high strength and modulus for use in engineering applications such as high performance composites, have undergone significant developments in the last two decades. One example has been the production of aromatic polyamides (aramids) such as poly(*p*-phenylene terephthalamide) (Kevlar or Twaron) which can be made by the spinning of liquid-crystalline solutions [1,2]. There are now several different grades of aramid fibres available commercially which may be produced by different routes to produce fibres with different mechanical properties [3]. There is now considerable interest in producing heterocyclic rigid-rod polymers [4,5], again by spinning from liquid-crystalline solutions. Heat-treated fibres of poly(*p*-phenylene benzobisthiazole) (PBT) have been produced with tensile modulus values of 320 GPa [4]. This may be compared with a value of 370 GPa obtained for poly(*p*-phenylene benzobisoxazole) (PBO) fibres [5].

Molecular deformation in high-performance fibres has been followed using Raman spectroscopy [6–10]. It has been found that well-defined Raman spectra are generally

obtained from high-modulus, high-strength polymer fibres. When such fibres are deformed, the frequencies of Raman active bands tend to decrease by an amount,  $\Delta\nu$ , dependent upon the material, the band under consideration and the modulus of the material. Similar behaviour has been found for a wide variety of high-performance fibres such as aromatic polyamide [6], PBT [7], PBO [8], polyethylene [9] and carbon fibres [10]. Recently, the Raman technique has been employed to also study the compressive properties of liquid crystalline polymer fibres [11–13]. The stress-induced Raman band shifts can be used to monitor the variation of fibre stress in both tension and compression.

In this present study the tensile and compressive molecular deformation of a new rigid-rod polymer fibre with strong hydrogen bonds between polymer chains, polypyridobisimidazole (PIPD or M5) [14] based on the structure as shown below:



have been examined using Raman spectroscopy. The mechanical properties of the fibres, in particular Young’s

\* Corresponding author.

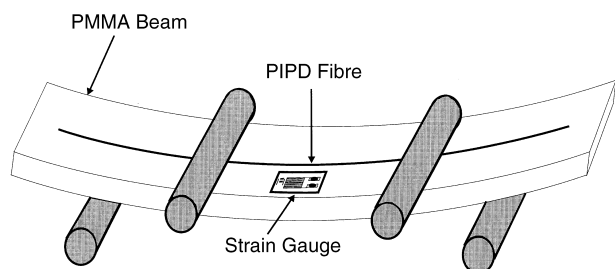


Fig. 1. Schematic diagram of the four-point bending arrangement used for deforming the M5 fibres in compression.

modulus and tensile strength, have also been determined and the molecular deformation processes investigated in detail.

## 2. Experimental procedure

### 2.1. Materials

The PIPD fibres used in this study coded M5-1 and M5-2 were supplied by Akzo Nobel Central Research, The Netherlands. The polymer was synthesized by Akzo Nobel Research and the fibres were spun from liquid crystalline solutions. They were also given different heat treatments after spinning to improve their mechanical properties and the two different fibres had been produced differently to produce slightly different structures and properties.

### 2.2. Mechanical testing

The Young's modulus, tensile strength, and failure strain were determined using a single-filament tensile testing. Individual PIPD fibres were mounted across holes on paper cards using a slow-setting, cold-curing epoxy resin adhesive which was left to cure for at least 5 days before

Table 1

The experimental values of the mechanical properties for the PIPD fibres

PIPD fibres	Gauge length (mm)	Young's modulus (GPa)	Tensile strength (GPa)
M5-1	20	$166 \pm 12$	$3.37 \pm 0.32$
	50	$234 \pm 18$	$3.12 \pm 0.30$
	100	$256 \pm 11$	$2.64 \pm 0.38$
M5-2	20	$151 \pm 17$	$3.86 \pm 0.15$
	50	$258 \pm 21$	$3.64 \pm 0.21$
	100	$293 \pm 18$	$3.11 \pm 0.20$

Table 2

The corrected values of the mechanical properties for the PIPD fibres

Mechanical properties	M5-1	M5-2
Young's modulus (GPa)	$279 \pm 18$	$328 \pm 21$
Tensile strength (GPa)	$3.80 \pm 0.20$	$4.06 \pm 0.60$
Failure strain (%)	$1.52 \pm 0.07$	$1.44 \pm 0.14$

testing. The paper cards were mounted between the grips of an Instron 1121 mechanical testing machine. The edges of the cards were cut and the load–displacement curves were recorded on chart paper. Gauge lengths of 20, 50 and 100 mm were employed with at least 10 specimens tested at each gauge length. Load ranges of 1 N and cross-head speeds of 0.2, 0.5 and 1 mm/min, were chosen giving a constant strain rate of  $0.01 \text{ min}^{-1}$ . All tests were carried out at  $23 \pm 2^\circ\text{C}$  and a relative humidity of  $50 \pm 5\%$ .

Individual PIPD fibres were examined in a Philips 505M scanning electron microscope (SEM) operated at 10 kV with its magnification calibrated using a calibration specimen set with 2160 lines/mm. A S150B Sputter Coater, operated at 1 kV and 40 mA for 2 min, was employed to coat the PIPD fibres with a thin layer of gold to avoid charge build-up during SEM operation. The diameters of the gold-coated

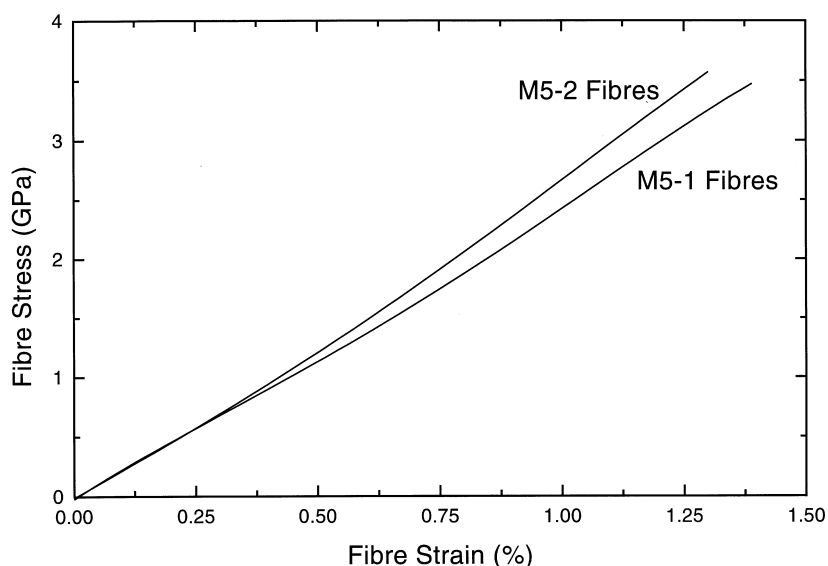


Fig. 2. A typical stress–strain curve for the PIPD fibres.

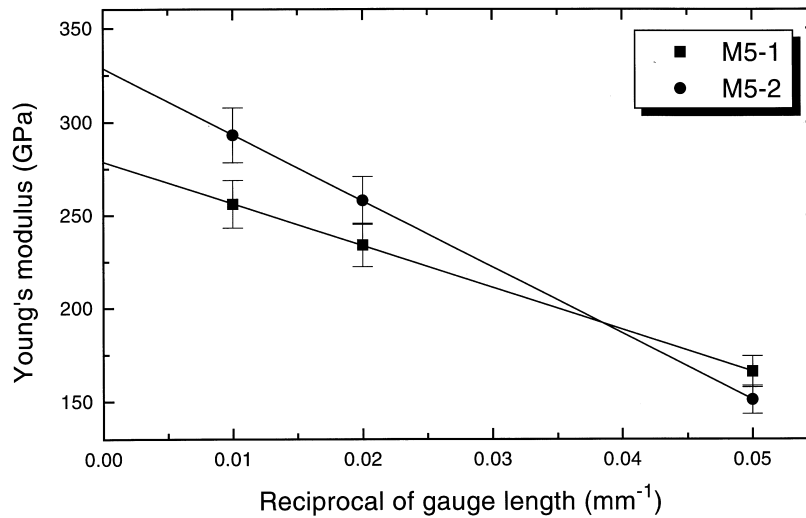


Fig. 3. Dependence of the Young's modulus upon the reciprocal of the fibre gauge length for the PIPD fibres.

fibres were then measured using the SEM and the average fibre diameters were determined from at least 25 measurements of fibre diameter. Kink bands along the fibres were also observed using the same SEM.

### 2.3. Raman spectroscopy

Raman spectroscopy was carried out using a Renishaw 1000 system. A Helium–Neon (He–Ne) laser was used giving a monochromatic red light of 632.8 nm at a power of approximately 1 mW. The 50 × objective lens of an Olympus BH-2 optical microscope is used both to focus the laser beam on the specimen and to collect the scattered radiation. The laser beam was polarized parallel to the fibre axis and focused to give a spot size of  $\sim 2 \mu\text{m}$  diameter on the fibre surface. A highly sensitive Renishaw Charge-Coupled Device (CCD) camera was used to collect the Raman spectra. The band intensity and band position were analysed using a Lorentzian curve-fitting procedure.

### 2.4. Raman deformation measurements

Spectra were obtained from PIPD fibres during deformation in a straining rig which fitted directly onto the microscope stage. Individual fibres were fixed between aluminium foil tabs which were placed onto the aluminium blocks of the straining rig using a cyanoacrylate adhesive, giving gauge lengths of approx. 50 mm. The fibres were deformed by displacing the blocks accurately using a micrometer attachment which could be read to  $\pm 0.005 \text{ mm}$ . This allowed a precision of the order of  $\pm 0.05\%$  for strain measurement. Raman spectra were obtained during deformation by scanning the peak position of the  $1507 \text{ cm}^{-1}$  Raman band for 25 s between loading steps of  $2 \mu\text{m}$  and at least five tests were carried out for each type of fibre.

Raman spectra were also obtained from single PIPD fibre specimens using a single-fibre stressing rig containing load cell to read the applied load. Individual fibres were fixed using cyanoacrylate adhesive between aluminium foil tabs

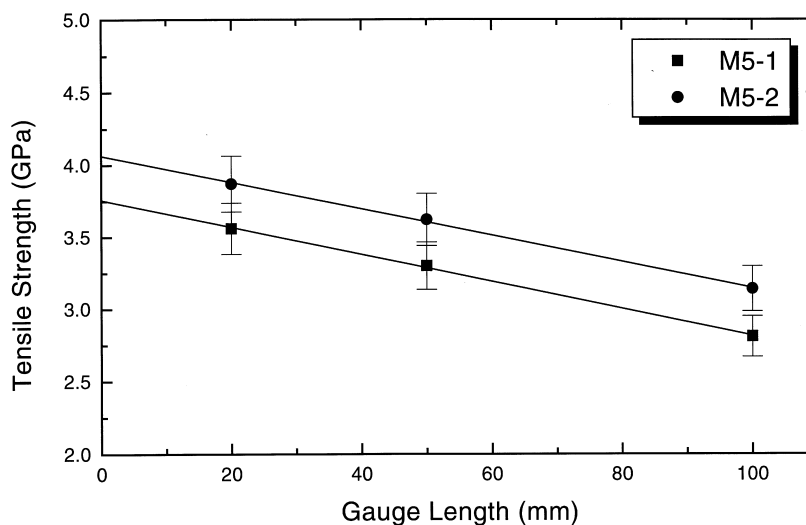


Fig. 4. Dependence of the tensile strength upon gauge length for the PIPD fibres.

and the load cell of the stress rig. A 50 mm gauge length specimen was again employed. The peak position of the  $1507\text{ cm}^{-1}$  Raman band was scanned for 25 s to give the Raman spectra during deformation in steps of  $2\text{ }\mu\text{m}$  and five specimens were tested for each type of fibre.

The peak position of the  $1507\text{ cm}^{-1}$  band was also followed from the Raman spectra recorded along PIPD fibres adhering to the surface of a beam in the four-point bending rig (Fig. 1). The four-point bend specimens used to study tensile and compressive deformation of the PIPD fibres were prepared using poly(methyl methacrylate) (PMMA) strips approximately 2 mm thick. An individual PIPD fibre was placed on the surface of the PMMA and covered with a thin layer of PMMA/chloroform solution which was allowed to dry. A resistance strain gauge with a gauge factor of 2.065 was centrally bonded to the surface of the PMMA

beam next to the fibre using cyanoacrylate adhesive and left to set for at least 5 days before testing.

Deformation was undertaken in both compression, in increments of  $-0.012\%$  compressive strain up to  $-0.7\%$  strain, and in tension with increments of  $0.012\%$  strain up to  $0.7\%$  strain. An exposure time of 10 s was used to obtain the Raman spectra.

### 3. Results and discussion

#### 3.1. Mechanical testing

The average diameters obtained from the SEM method were used for the calculation of Young's moduli and tensile strengths. The average values of diameter determined were

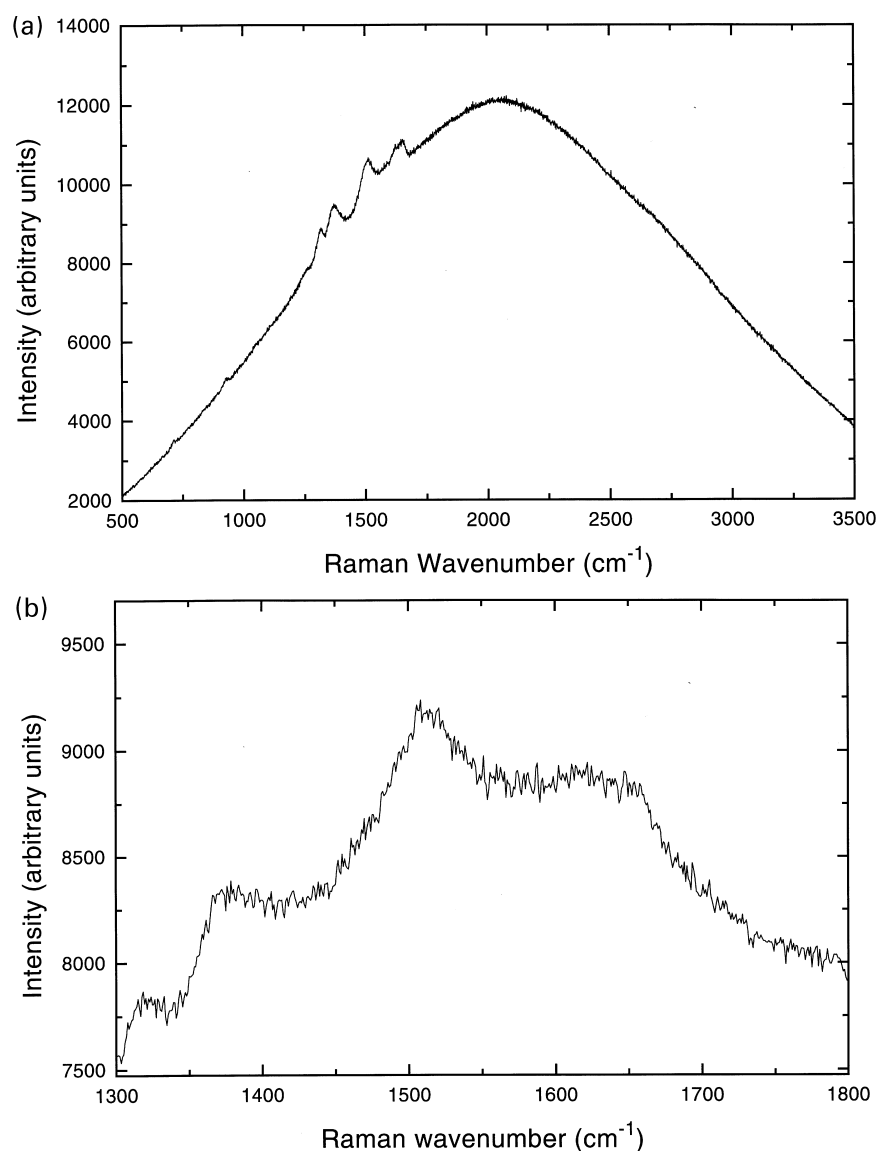


Fig. 5. Typical Raman spectra obtained from a single filament of a PIPD fibre using a low power He–Ne laser. (a) The  $500\text{--}3500\text{ cm}^{-1}$ ; and (b)  $1300\text{--}1800\text{ cm}^{-1}$  regions.

$11.4 \pm 1.4 \mu\text{m}$  and  $12.2 \pm 0.9 \mu\text{m}$  for the M5-1 and M5-2 fibres, respectively.

The stress–strain curves shown in Fig. 2 for both types of PIPD fibre are approximately linear up to fracture and do not appear to yield. It appears that there is a slight strain hardening at higher strains as found in aramids [15]. This is because the application of tension leads to an improvement in orientation of the fibre structure, resulting in the increasing slope of the stress–strain curve [16].

Additionally, the results showed that the Young’s modulus increases with increasing gauge length, as shown in Table 1. This is thought to be due to end effects which have an influence on the true gauge length during the test [17]. The end effects, which are due to difficulties in defining the exact gauge length, are greater for shorter gauge lengths leading to an apparent reduction in the Young’s modulus.

Machine softness of the gripping system is one of the major problems which causes errors in determination of fibre extension, especially for short specimens, resulting in higher failure strains. The corrected value of the modulus (Table 2) can therefore be obtained by plotting the Young’s modulus of the fibres versus the reciprocal of the gauge length and then extrapolating to infinite gauge length, as shown in Fig. 3.

The experimental values of tensile strength listed in Table 1 were found to decrease with increasing gauge length. This is because the longer the gauge length, the greater the probability of encountering defects such as flaws in the fibres and thus the lower the tensile strength. Moreover, further variation of the results was due to fibre slippage and specimen preparation which may cause fibre pre-stretching. The variation of the tensile strength with gauge length is plotted for the PIPD fibres in Fig. 4

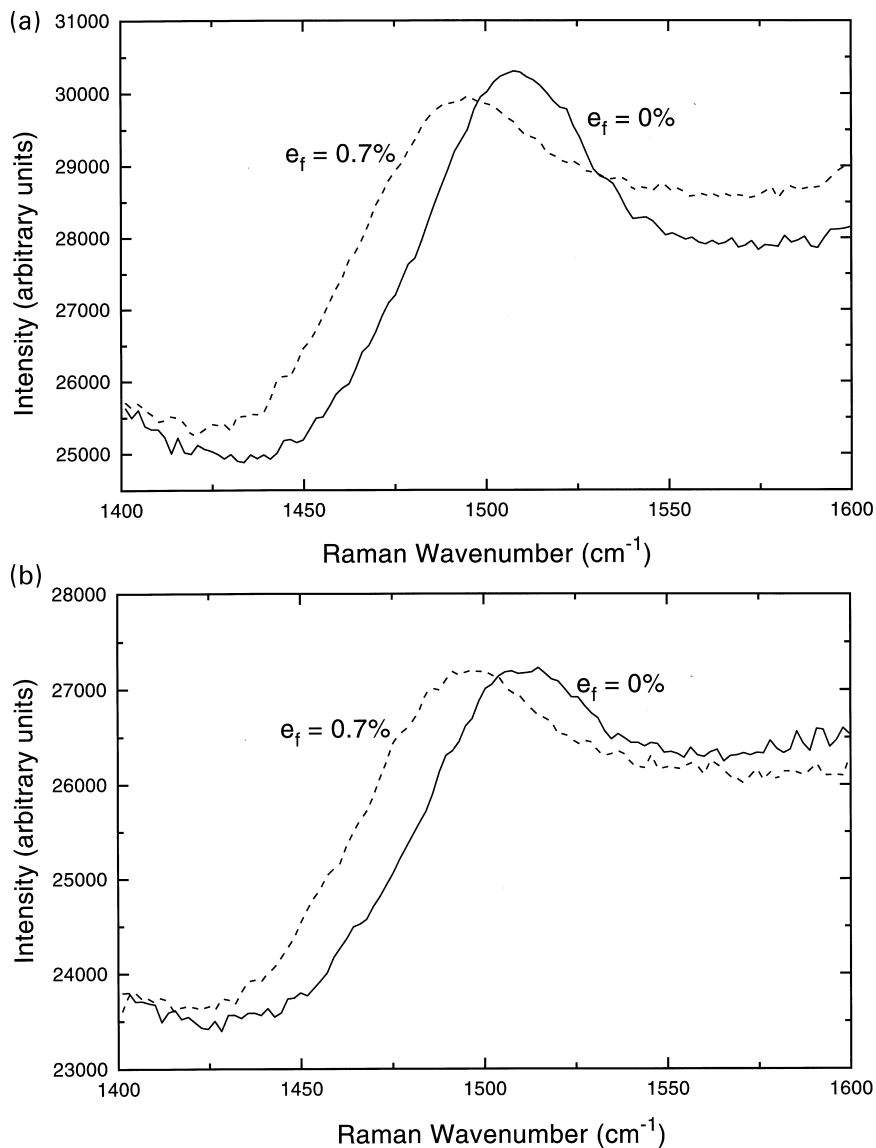


Fig. 6. Raman spectra in the region of the  $1507 \text{ cm}^{-1}$  band obtained at strains of 0% and 0.7% showing the peak position shift for the PIPD fibres (a) M5-1; (b) M5-2.

which shows linear behaviour. Estimations of the corrected tensile strengths (Table 2) can be obtained by extrapolating to zero gauge length for elimination of the effect of the presence of defects, as shown in Fig. 4.

### 3.2. Raman spectroscopy and deformation studies

A typical Raman spectrum which is identical for the two types of PIPD fibre in the region of  $500\text{--}3500\text{ cm}^{-1}$  is shown in Fig. 5a. The spectrum consists of a few well-defined intense peaks on a strong fluorescent background. Four principle Raman bands on the fluorescent background in the region  $1300\text{--}1800\text{ cm}^{-1}$  are clear in the Raman spectra of the PIPD fibres, as illustrated in Fig. 5b. These bands are located approximately at  $1320$ ,  $1380$ ,  $1507$  and  $1620\text{ cm}^{-1}$  with the  $1507\text{ cm}^{-1}$  band being the most intense band and therefore chosen to follow deformation. Although band assignments have not been made for the PIPD fibres, it

is likely that the  $1507\text{ cm}^{-1}$  band is due principally to  $\text{-C}=\text{N-}$  stretching vibration using the analogy of the  $1505\text{ cm}^{-1}$  band in PBT fibres and the  $1550\text{ cm}^{-1}$  band in PBO fibres [18].

The effect of deformation upon the peak position for the  $1507\text{ cm}^{-1}$  band is shown in Fig. 6a and Fig. 6b for the two PIPD fibres. It is evident that the band at  $1507\text{ cm}^{-1}$  shifts to lower frequency on the application of tensile strain,  $e_f$ . Shifts of the vibrational frequencies in particular Raman-active band in high performance fibres are thought to be due to a distortion of the backbone covalent bonds caused by mechanical deformation [19].

It can also be seen in Fig. 7 and Fig. 8 that each fibre exhibits a linear shift in the Raman wavenumber with applied stress or strain until failure of the fibre takes place. This is entirely consistent with the fibre stress–strain behaviour, where the stress–strain curve is approximately linear up to failure. The stress and strain sensitivities

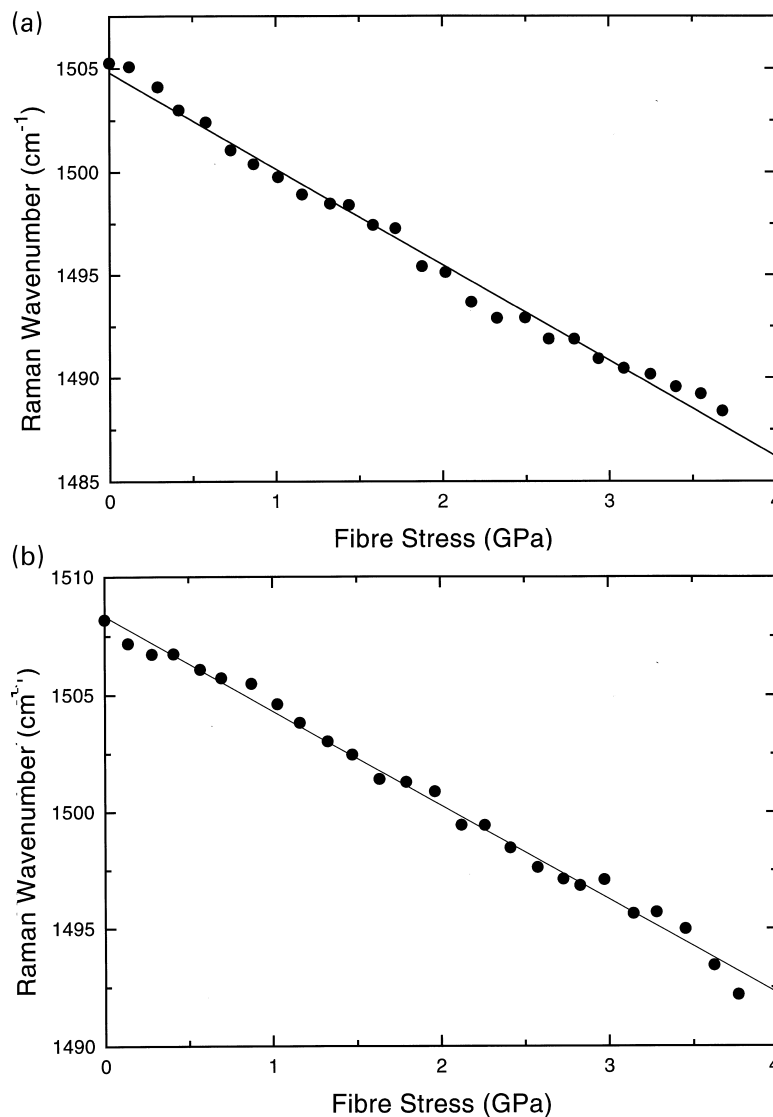


Fig. 7. Variation of the peak position of the  $1507\text{ cm}^{-1}$  with tensile fibre stress for the PIPD fibres (a) M5-1; and (b) M5-2 (gauge length = 50 mm).

Table 3  
Stress and strain sensitivities ( $\pm$  standard deviations) of the  $1507\text{ cm}^{-1}$  Raman band for fibres (average of five nominally identical specimens of 50 mm gauge length)

PIPD fibres	Stress sensitivity ( $\text{cm}^{-1}/\text{GPa}$ )	Strain sensitivity ( $\text{cm}^{-1}/\%$ strain)
M5-1	$-4.0 \pm 0.5$	$-15.3 \pm 1.5$
M5-2	$-4.3 \pm 0.5$	$-16.5 \pm 0.7$

obtained from the slope of these lines for the  $1507\text{ cm}^{-1}$  band are listed in Table 3, indicating that there is no significant difference in the rate of shifts between the two types of PIPD fibre.

It should be pointed out that there is a large change in the Raman frequency at a given level of stress and strain for the M5 fibres. The reason for this is that the high fibre modulus due to a high degree of orientation of inherently stiff molecules leads to the polymer molecules taking higher levels of

stress at a given strain, which results in a considerable Raman band shift. In addition, tensile properties of the fibres calculated from the Raman data are comparable with those obtained from mechanical testing showing that the Raman technique is very effective for studying both the molecular deformation process and undertaking conventional single fibre deformation. This is because the shift of the Raman upon the application of macroscopic stress or strain is due to molecular deformation such as chain stretching in the PIPD polymer fibres.

### 3.3. Compressive deformation

The compressive deformation of the PIPD fibres was followed using SEM as shown in Fig. 9 and kink bands were found to form along the fibres when they were subjected to bending deformation. They were found to form at various angles to the fibre axis as a region of plastic shear

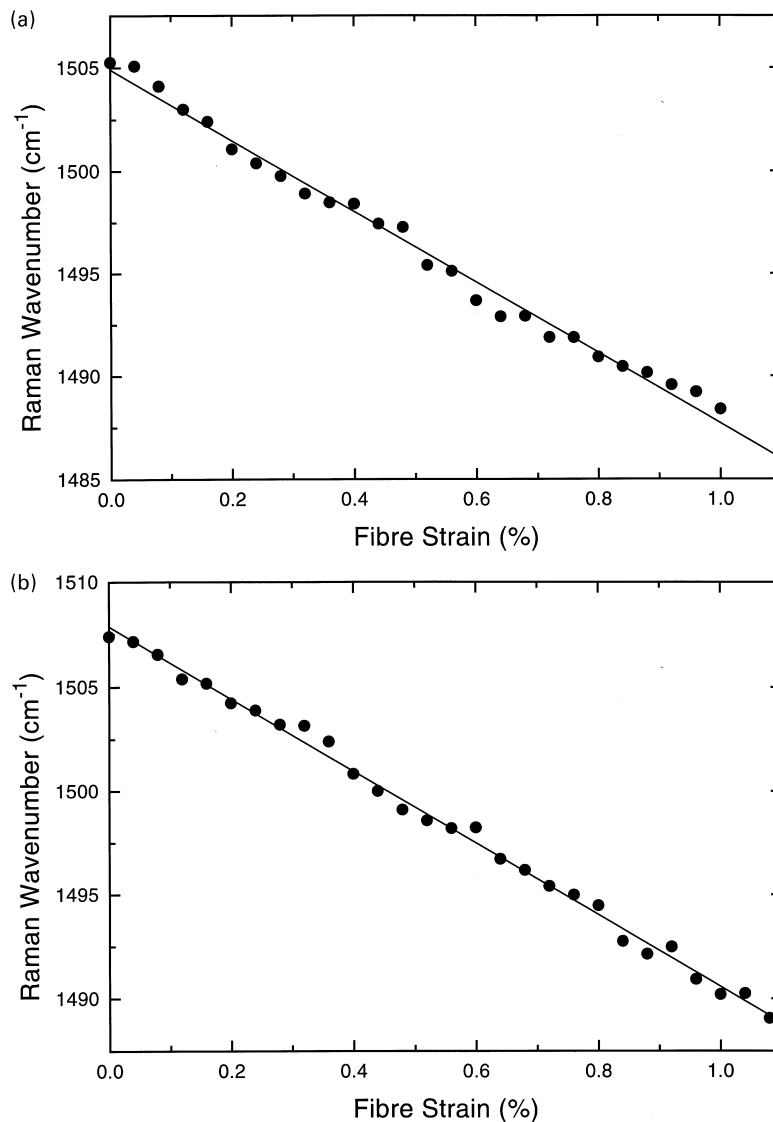


Fig. 8. Variation of the peak position of the  $1507\text{ cm}^{-1}$  with tensile fibre strain for the PIPD fibres: (a) M5-1; and (b) M5-2 (gauge length = 50 mm).

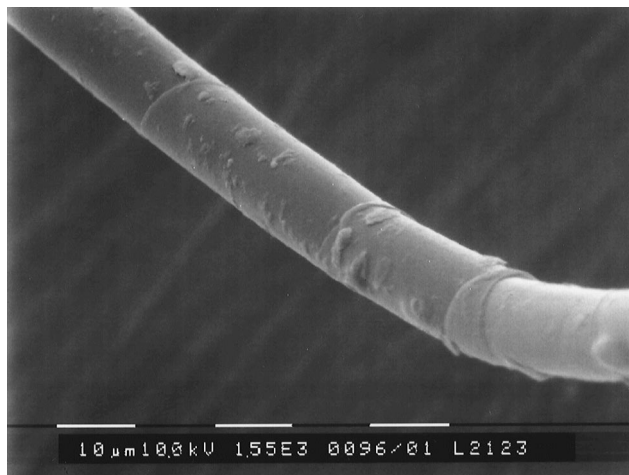


Fig. 9. SEM micrograph for a kink band observed along a PIPD fibre.

deformation leading to a large change in orientation of the molecules within the fibres [20]. The kink bands shown in Fig. 9 are similar to those seen in other high-performance polymer fibres [20], although in the case of PIPD fibres they only formed after fibres were subjected to significant levels of bending.

The Raman technique was also employed in order to study the compressive properties which can be observed for both of the PIPD fibres using a four-point bending test that provides uniform strain between the loading points [13]. The peak positions of the  $1507\text{ cm}^{-1}$  Raman band for single PIPD fibres at 0%, +0.3% tensile and -0.3% compressive strains are shown in Fig. 10a and Fig. 10b. It can be seen that the bands shift to lower frequency in tension and to higher frequency in compression, as has been found in other high performance fibres [6,11–13,21,22].

In this study the PIPD fibres were deformed in both

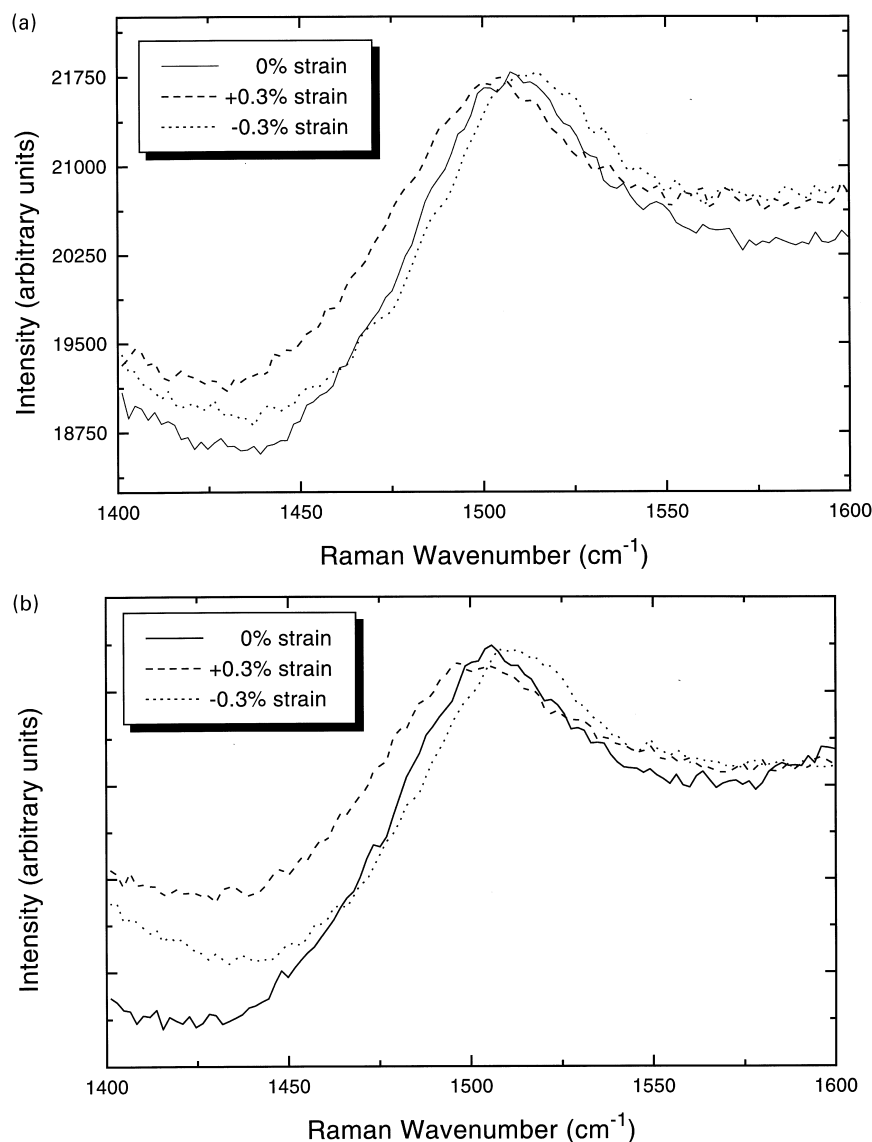


Fig. 10. The position of the  $1507\text{ cm}^{-1}$  band obtained from PIPD fibres at 0%, +0.3% tensile and -0.3% compressive strain: (a) M5-1; and (b) M5-2.



Table 4  
Calculated compressive properties for the PIPD fibres using the four-point bending test

High-performance polymer fibres	Compressive strength (GPa)
M5-1	$0.99 \pm 0.30$
M5-2	$0.85 \pm 0.21$
Aramid[13,20]	0.35–0.45
PABI[20]	0.42
PBO[20]	0.2–0.4
PBZT[20]	0.3–0.4

Average of three fibres for each material. Values of compressive strength for other high-performance polymer fibres are also listed.

tension and compression up to  $\pm 0.7\%$  strain. The variations of the peak positions of the  $1507\text{ cm}^{-1}$  bands with tensile and compression fibre strain for the two types of fibre are presented in Fig. 11a and Fig. 11b. It can be seen

that there is an approximately linear relationship between band position and fibre strain when the fibres are deformed in tension. In compression, however, the same peak shifts to higher frequency linearly with increasing fibre strain until it reaches a maximum value, then decreases slightly and eventually maintains a plateau value. This behaviour is not unlike that found for aramid fibres [13], although in the case of aramid fibres there is a tendency for the slope of the line to decrease with increasing compressive strain and the maximum to be less well defined. It was found using optical microscopy [23] that the maximum in the Raman band shift for the PIPD fibres corresponded to the onset of kink band formation, and the plateau to the formation of further kink bands along with the thickening of the original ones.

By using the rates of shift of the  $1507\text{ cm}^{-1}$  band with stress for the M5-1 and M5-2 fibres from Table 3, it is possible to derive from the data in Fig. 11 the full

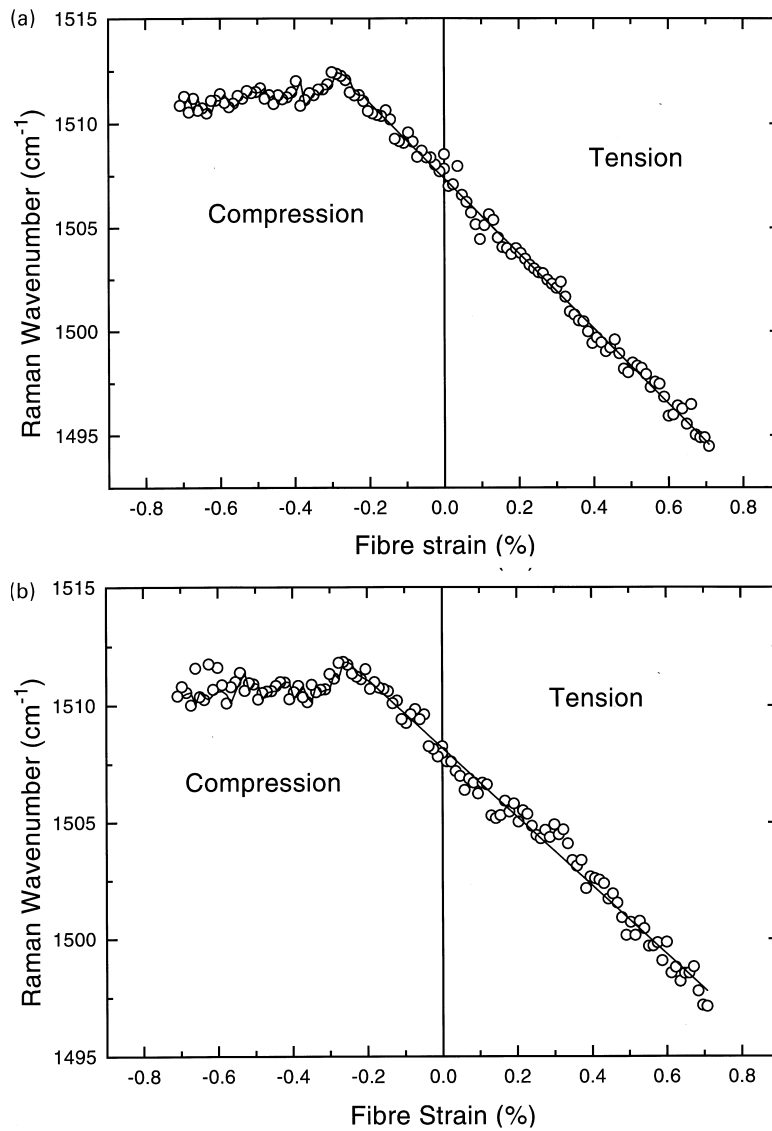


Fig. 11. Variation of the peak position of the  $1507\text{ cm}^{-1}$  band with fibre strain for PIPD fibres deformed in both tension and compression: (a) M5-1; and (b) M5-2.

stress–strain curves for the PIPD fibres shown in Fig. 12. From these stress–strain curves it is possible to calculate the maximum compressive stress in the fibres which can be assumed to be their compressive strength (Table 4). It should be noted also that the slopes of the lines in Fig. 12a and Fig. 12b are essentially the same within the limits of experimental error, indicating that, to a first approximation, the fibres have the same modulus in tension and compression.

It should be pointed out that the compressive strength of the PIPD fibres, determined by the four-point bending method, is higher than those of other high performance polymer fibres also listed in Table 4 which normally range between 200 and 450 MPa [13,20], indicating that the fibres are able to resist compressive deformation more efficiently than other polymer fibres. In addition, the similar modulus in tension and compression is unusual for high-performance polymer fibres where some strain

softening is found during compressive deformation [13]. The reason for the superior compressive behaviour of the PIPD fibres is due to the presence of polar -NH, -OH groups on molecules leading to strong interchain H-bonding in different directions perpendicular to the polymer backbone [14]. This improves compressive behaviour by stopping molecules sliding past each other during compressive deformation [20]. The behaviour of the PIPD fibres should be compared with PBO or PBT rigid-rod polymer fibres (Table 4) where the lack of intermolecular forces between the polymer chains leads to significantly lower levels of compressive strength.

#### 3.4. Applications in composites

The superior compressive properties of the PIPD fibres makes them attractive for use as reinforcing fibres in high-performance polymer-fibre reinforced composites

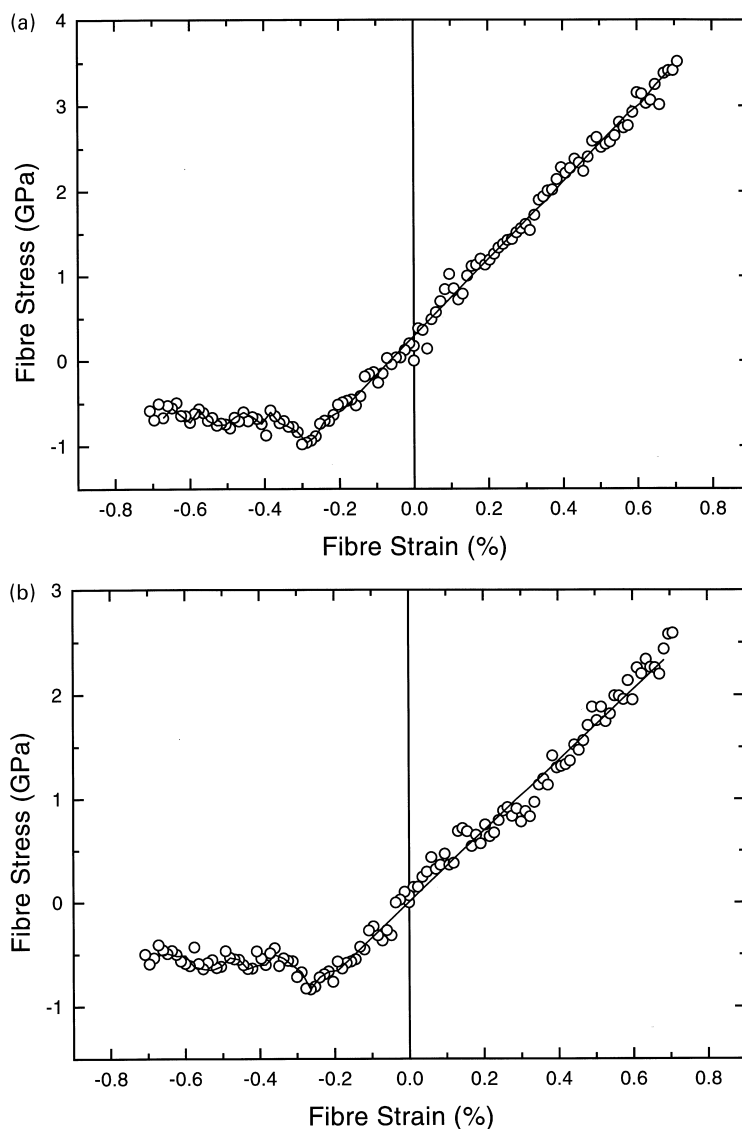


Fig. 12. Derived variation of fibre stress with fibre strain for PIPD fibres deformed in both tension and compression: (a) M5-1; and (b) M5-2.

where problems are often encountered because of the low levels of compressive strength of most polymer fibres. The compressive properties of such fibres are reflected in the poor compressive behaviour of the composite [24]. In fact, it has been suggested [14] that the mechanical behaviour of the PIPD fibres is more like that of carbon fibres than of polymer fibres. Another aspect of PIPD fibres that makes them good candidates for reinforcement applications is that they show good adhesion with polymer matrix materials such as epoxy resins without the need for the use of any special adhesion promoters [14]. It was found in this present study that there was good adhesion between the fibres and epoxy resin adhesive used in the mechanical testing of the fibres, whereas slippage due to poor adhesion is often encountered with other high-modulus fibres.

#### 4. Conclusions

It has been shown that the new aromatic rigid-rod PIPD or M5 polymer fibres, have mechanical impressive properties. The Young's modulus and tensile strength have been found to be greater than 300 GPa and 4 GPa, respectively, and there is some evidence of slight strain hardening in the stress–strain curves at high strains. Raman spectroscopy has been proven to be a successful technique to study deformation of the PIPD fibres on a molecular level. The 1507  $\text{cm}^{-1}$  Raman band shifts to lower wavenumber with applied strain at the rate of  $-15.3 \pm 1.5 \text{ cm}^{-1}/\%$  strain for the M5-1 fibres and by  $-16.5 \pm 0.7 \text{ cm}^{-1}/\%$  strain for the M5-2 fibres. Tensile stress also induces the 1507  $\text{cm}^{-1}$  Raman band to shift to lower wavenumber by  $-4.0 \pm 0.5 \text{ cm}^{-1}/\text{GPa}$  and  $-4.3 \pm 0.5 \text{ cm}^{-1}/\text{GPa}$  for the M5-1 and M5-2 fibres, respectively. Furthermore, the same Raman band has been found to shift to higher wavenumber in compression with no evidence of strain softening in the PIPD fibres. The compressive moduli for the PIPD fibres have also been found to be greater than 300 GPa with compressive strengths of up to 1 GPa which is considerably higher than for any other high-performance polymer fibre. It appears that the high level of compressive strength combined with their good adhesion with matrix resin materials makes PIPD fibres strong candidates for use in high-performance polymer-fibre reinforced composites.

#### Acknowledgements

One of the authors (RJY) would like to thank the Royal Society for support in the form of the Wolfson Research Professorship in Materials Science. The other (JS) is grateful to the Government of Thailand for financial support. The PIPD fibres were kindly supplied by Akzo Nobel Central Research. The work forms part of a large programme of research supported by the Engineering and Physical Sciences Research Council.

#### References

- [1] Allen SR, Fillippov AG, Farris RJ, Thomas EL. In: Zachariades AE, Porter RS, editors. *Strength and stiffness of polymers*. New York: Marcel Dekker, 1983.
- [2] Yang HH. *Aromatic high-strength fibres*. Chichester, UK: Wiley, 1989.
- [3] Kwolek SL, Memeger W, Van Trump JE. In: Lewin M, Preston, J, editors. *High technology fibres—Part B*. New York: Marcel Dekker, 1989.
- [4] Allen SR, Farris RJ, Thomas EL. *J Mater Sci* 1985;20:2727.
- [5] Krause SJ, Haddock TB, Vezie DL, Lenhart PG, Hwang WF, Price GE, Helminiak TE, O'Brien JF, Adams WW. *Polymer* 1988;29:1354.
- [6] Young RJ, Lu D, Day RJ, Knoff WF, Davis HA. *J Mater Sci* 1992;27:5431.
- [7] Day RJ, Robinson IM, Zakikhani M, Young RJ. *Polymer* 1987;28:1833.
- [8] Young RJ, Day RJ, Zakikhani M. *J Mater Sci* 1990;25:127.
- [9] Wong WF, Young RJ. *J Mater Sci* 1994;29:510.
- [10] Huang Y, Young RJ. *J Mater Sci* 1994;29:4027.
- [11] Vlatts C, Galiotis C. *Polymer* 1991;32:1788.
- [12] Vlatts C, Galiotis C. *Polymer* 1994;35:2335.
- [13] Andrews MC, Lu D, Young RJ. *Polymer* 1997;38:2379.
- [14] Sikkema DJ. *Polymer*, in press.
- [15] Northolt MG. *Polymer* 1980;21:1199.
- [16] Morton WE. *Physical properties of textile fibres*. Manchester: The Textile Institute, 1993.
- [17] Jones JB, Barr JB, Smith RE. *J Mater Sci* 1980;15:2415.
- [18] Venkatesh GM, Shen DY, Hsu SL. *J Polym Sci, Polym Phys* 1981;19:1475.
- [19] Young RJ, Day RJ, Ang PP. *Polymer Commun* 1990;31:47.
- [20] Kozey VV, Jiang H, Mehta VR, Kumar S. *J Mater Res* 1995;10:1044.
- [21] Andrews MC, Day RJ, Hu X, Young RJ. *Comp Sci and Tech* 1993;48:255.
- [22] Melanitis N, Galiotis C. *J Mater Sci* 1990;25:5081.
- [23] Sirichaisit J. MSc Dissertation, UMIST, 1997.
- [24] Andrews MC, Young RJ, Mahy J, Schaap AA, Grabandt O. *J Comp Mater* 1998;32:803.